Measurement of Individual Structure-Factor Phases with Tenth-Degree Accuracy: the 00.2 Reflection in BeO Studied by Electron and X-ray Diffraction

By J. M. Zuo and J. C. H. Spence

Department of Physics, Arizona State University, Tempe, AZ 85287, USA

J. Downs

Department of Geological Sciences, The Ohio State University, 291 Watts Hall, 2041 College Road, Columbus, OH 43210, USA

and J. Mayer

Max-Planck Institut für Metallforschung, Institut für Werkstoffwissenschaft, Seestrasse 92, D-7000 Stuttgart 1, Germany

Abstract

Measurements of the phase (and amplitude) of the 00.2 structure factor of BeO are reported. These were obtained by applying an automated least-squares refinement method to experimental convergent-beam transmission electron diffraction data, collected from sub-micrometer single-crystal regions of two different thicknesses. Multiple-scattering effects were included, using the Bloch-wave method. Perturbation methods were used to include weak beams and to estimate errors. After conversion to X-ray structure factors, it was found that $\varphi^x(00.2) = -1.190\,(9)$ rad. The same value was found, within experimental error, using data collected from a region of different thickness. New single-crystal X-ray results are also reported, which are in good agreement with the electron diffraction results. Phases derived from multipole refinement using X-ray data are about fifty times less accurate than the electron results. This electron diffraction technique may be the most accurate method for the measurement of low-order structure-factor phases from acentric crystals with small unit cells. The method may therefore allow the extension of previous highly accurate studies of charge density in silicon to acentric materials from which large single crystals cannot be grown.

1. Introduction

In recent years, many papers have appeared devoted to the theory of struture-factor phase measurements in acentric crystals by X-ray diffraction (Chang, 1987; Thorkildsen, 1987; Shen & Collela, 1988; Weckert & Hummer, 1990). A parallel effort in the field of theoretical electron diffraction has also recently made rapid progress (Marthinsen & Høier, 1986, 1988; Bird & James, 1988; Zuo, Høier & Spence, 1989; Zuo, Spence & Høier, 1989). On the experimental side, progress has been slower but several experimental measurements have now been published of the phases of low-order structure-factor phases in acentric crystals by both techniques. The experimental X-ray methods currently lack accuracy [phases are typically determined to within about 45° (Hümmer, Weckert & Bondza, 1990)] but may readily be applied to organic crystals with large unit cells and, by use of synchrotron radiation, are potentially capable of rapidly processing large numbers of reflections. The electron diffraction results are far more accurate (typically within 1° (Zuo, Spence & Høier, 1989; see also this work) but are so far restricted to inorganic crystals of known structure and have yet to be extended to large unit cells or unknown structures. The electron diffraction work may analyse sub-micrometer- (or even sub-nanometer-sized) regions of a crystal and may be combined with atomic-resolution electron-microscope imaging of the same region and is thus free of problems due to defects. The transmission (Laue) geometry is always used. Count rates may be as high as 1 MHz. The accuracy obtainable in the electron diffraction work is sufficient to provide information on bonding in acentric crystals of known structure, whereas the X-ray work is more useful in providing constraints for structure analysis in large-unit-cell crystals. The similarity of approach in the X-ray and electron work is striking, although there appears to be little communication between researchers in the two fields. Three-beam methods are popular in both fields. In particular, our previous nonsystematics work (Zuo, Høier & Spence, 1989) corresponds to a study of the Renninger effect in X-ray diffraction. In both fields it has proved possible to determine not only the magnitudes of three-phase structure invariants but also their signs (Marthinsen & Høier, 1989; Hümmer *et al.*, 1990).

The first phase measurement for an acentric crystal using electron diffraction appears to be that of Ichimiya & Uyeda (1977). Reviews of phase measurement are given by Chang (1987) for X-ray diffraction and Cowley (1992) and Zuo, Høier & Spence (1989) for electron diffraction. A general review of structure-factor measurement by electron diffraction is given by Spence (1993).

This progress in electron crystallography has occurred as a result of advances in instrumentation, computing power and theory. Whereas it was shown by Kambe (1957) that three-beam dynamical intensities depend on an origin-independent sum of phases, detailed treatments of the three-beam case in acentric crystals have appeared only recently (Marthinsen & Høier, 1986, 1988; Marthinsen, Matsuhata, Høier & Gjonnes, 1988; Zuo, Høier & Spence, 1989). These closed-form solutions have indicated the regions in convergent-beam electron diffraction (CBED) patterns that are most sensitive to phases and also revealed the general trends in the behavior of the parameters. The high accuracy in measurement was also made possible by the development of fast computers, which allow many-beam dynamical computations to be repeated over a range of parameter values and hence allow phases to be refined in a similar way to structure-factor amplitudes. The recent development of energy filters for electron microscopes has also been indispensable for the attainment of high accuracy and the new generation of imaging ω filters (Mayer, Spence & Mobus, 1991), combined with charge-coupled-device detectors, promises greater efficiency.

Previous work has aimed at the measurement of three- (or two-) phase invariants. We take φ_g to be the phase of the electron structure factor U_g with respect to some origin. Thus, if beams h and g are simultaneously at the Bragg condition, the quantity

$$\Psi = -\varphi_g + \varphi_h + \varphi_{g-h}$$

is independent of the choice of origin in the crystal and may be measured. This is done by comparing many-beam computations with the experimental intensity along Bragg hyperbolas near a three-beam intersection in convergent-beam patterns (Zuo, Høier & Spence, 1989). Because the crystal is illuminated with a converging cone of radiation, these patterns reveal a complete rocking curve simultaneously in each diffracted order. A variant of the systematic critical-voltage method, modified for acentric crystals, has also been developed (Zuo, Spence & Høier, 1989). In this paper, we describe the measurement of the phase (and amplitude) of the 00.2 reflection in BeO using the method described by Zuo, Spence & Høier (1989) together with a new automated refinement algorithm. In the systematics critical-voltage method for acentric crystals, the crystal is tilted so that only reflections g and $2g$ in a systematic

row are strongly excited. The convergent-beam electron diffraction mode is used to obtain rocking-curve information for each reflection. The intensity in the rocking curve for reflection g (near the Bragg condition) is used for the refinement of the amplitude of the structure factor for reflection g. The intensity within the rocking curve for reflection $2g$ is sensitive to the two-phase invariant

$$\Psi = -2\varphi_g + \varphi_{2g}.$$

This is used for the refinement of the phase of the structure factor of reflection g, with the assumption that the phase of the $2g$ structure factor is known. Thus we measure a single phase rather than a three-phase invariant. The automated structure-factor refinement algorithm (Zuo & Spence, 1991) is applied here for the first time to a noncentrosymmetric crystal.

BeO has the wurtzite-$2H$ structure, space group $P6_3mc$, with cell parameters $a = 2.6979$ (2) and $c = 4.3772$ (2) Å (Downs, Ross & Gibbs, 1985). For the ideal wurtzite-$2H$ structure, $c/a = 1.633$ and the z parameter is 0.375. BeO is compressed along the c axis relative to this ideal; we have used $z = 0.3775$. We chose an origin at the light Be atom. The polarity of the crystal is defined as follows: a vector drawn from Be to O in the wurtzite-$2H$ structure is defined as the positive [00.1] direction. Previous X-ray measurements on BeO (Vidal-Valat, Vidal, Kurki-Suonio & Kurki-Suonio, 1987) have been used in a multipole analysis to suggest the formation of bonded hexagonal O^{2-} planes, making diffuse O–O bridges bent toward the Be ions. Some covalency was found in the character of the Be–Be bond between the oxygen planes. The structure-factor phases were refined iteratively and a separate study was made of the oxygen sublattice. Some anharmonicity was found in thermal vibrations along the hexagonal axis.

2. Experimental

The experimental data consisted of the electron intensity distribution $[00h]$ in convergent-beam electron diffraction (CBED) patterns from BeO. Reviews of the CBED technique are given by Cowley (1992) and Spence & Zuo (1992). The crystal is illuminated by a cone of radiation with semi-angle about equal to the Bragg angle. The transmission diffraction pattern thus consiststs of discs, which are rocking curves, presented simultaneously in several diffracted orders, each covering an angular range about twice the Bragg angle.

Crushed samples of single-crystal BeO were coated lightly with carbon to improve conductivity and collected on holey carbon grids. To avoid toxicity problems, the crushing was done under a fume hood in a laboratory specializing in Be compounds (Pulvermetallurgische Institut, Max-Planck Institut, Stuttgart). The crystal used was identical to that

previously studied by γ-ray diffraction and neutron diffraction (Downs, Ross & Gibbs, 1985). A Philips 400T electron microscope was used, operating at 80 kV and fitted with a Gatan serial electron-energy-loss spectrometer tuned to the elastic-scattering peak. This results in a large reduction in background that is otherwise present due to inelastic scattering. This spectrometer uses a photomultiplier and scintillator detector and so provides data with much greater dynamic range than parallel-detection spectrometers. CBED patterns were obtained at room temperature on film, while selected regions of the patterns were also scanned across the 1 mm entrance aperture to the spectrometer. A camera length of 6.0 m was used for the scans and the CBED patterns were obtained from regions of crystal approximately 45 nm in diameter and about 100 nm thick. The patterns recorded on film were used to index the patterns and to determine the approximate beam direction with respect to off-systematics reflections.

Data were collected along the $[00.h]$ systematics, with use of a PDP 11 computer to control deflection of the patterns over the spectrometer aperture and data acquisition. The dwell time was 0.05 s at each point. To minimize the effects of variations in electron-source intensity, scans were repeated five times, the average was taken and the variance was calculated for use in the error analysis (see error bars on data). Counts could also be taken and compared at reference points before and after a scan to check for source stability. A lanthanum hexaboride electron source was used and was found to give sufficient stability if the electron gun had recently been cleaned.

Fig. 1 shows a typical CBED pattern from BeO in the $[1\bar{1}.0]$ orientation, with the 00.1 reflection at the Bragg condition. The dark cross shows the locus of dynamically forbidden reflection along which all multiple-scattering paths cancel (Gjønnes & Moodie, 1965). Radial lines of absence, A, are obtained in every second reflection along $\mathbf{c}$, indicating a c glide if three-dimensional multiple scattering could be ensured. In addition, the first-order 00.1 reflection is at the Bragg condition and shows a band, B, of extinction across the c axis, indicating, for three-dimensional scattering, a 2_1 screw axis along $\mathbf{c}$. This is contained in the 6_3 screw element of the space group. From this figure alone, however, since it is in fact dominated by zero-order Laue-zone (ZOLZ)
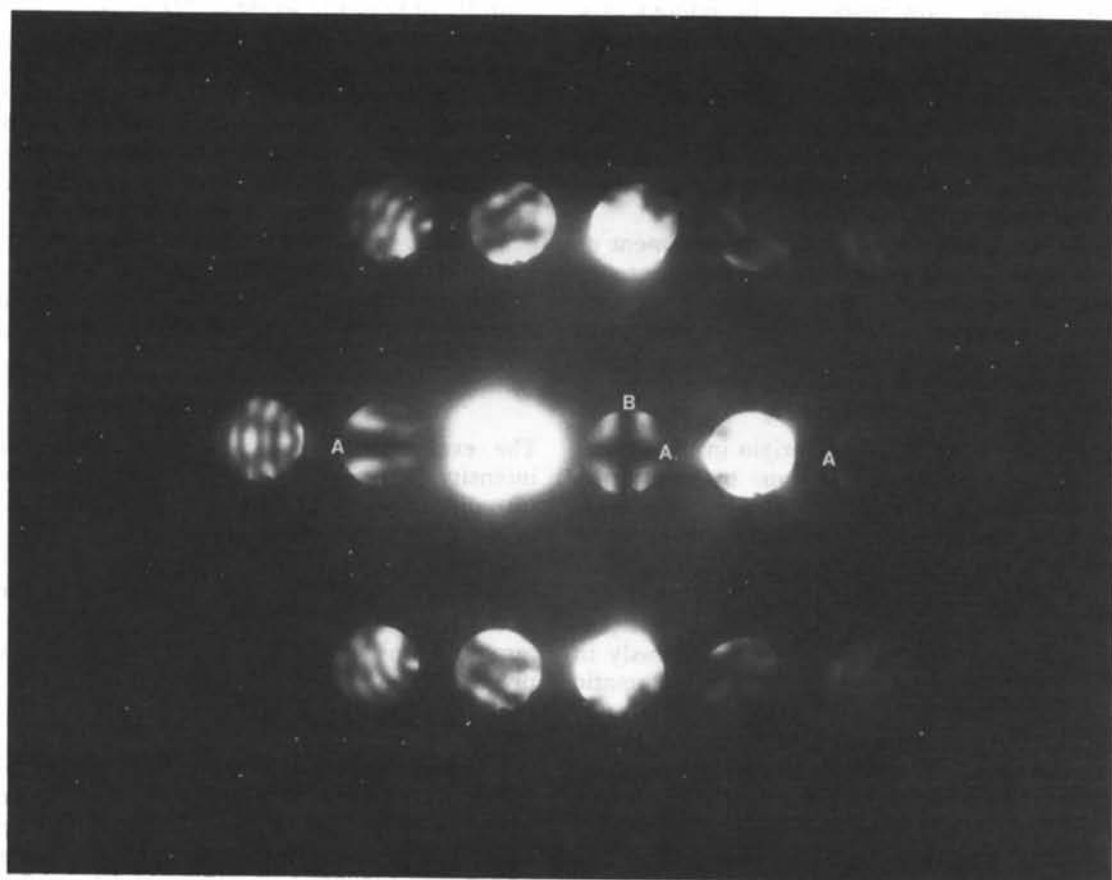

Fig. 1. BeO [1010] zone-axis convergent-beam electron diffraction pattern. Beam normal to c axis, with first-order reflection 0001 at the Bragg condition, showing Gjønnes–Moodie dark cross AB and dark radial lines A in every second order along the c axis.

scattering, we may conclude only that there exists either a screw axis along **c** or a **c** glide or both (Eades, 1988).
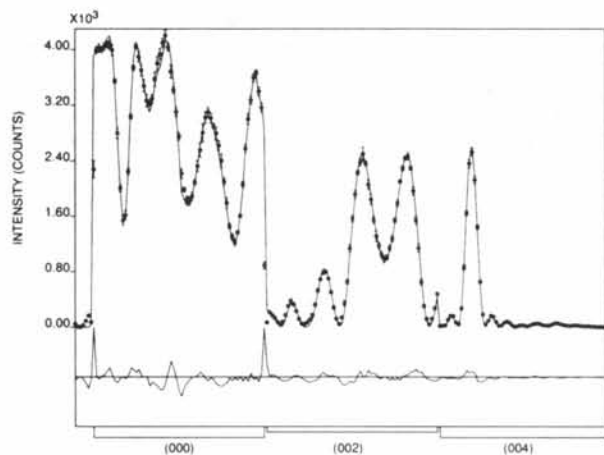

Fig. 2. Zero-loss energy-filtered experimental and computed CBED intensity along [00.2] in the central disc for BeO at 80 keV. The 00.2 and 00.4 Bragg conditions are indicated. The orientation is near the [13.0] zone axis. Refined sample thickness $t = 709.29$ Å. The plot below shows the difference between calculation and experiment.

Fig. 2 shows the data used to refine the complex structure factor $U(00.2)$ and the absorption coefficient $U'(00.2)$. The CBED pattern was tilted slightly to bring both the 00.2 and 00.4 reflections to the Bragg condition at the same setting and then rotated about the systematics line to a sparse zone. Fig. 3 shows the orientation chosen, near the [$\bar{1}$3.0] zone axis. This sparse zone minimizes off-systematics reflections, while including the 00.h reflections of interest. Fig. 4 shows data for a similar orientation but different crystal thickness, also at 80 kV.

3. Data analysis

The algorithm used is described in detail elsewhere (Zuo & Spence, 1991). It consists of a many-beam Bloch-wave multiple-scattering program coupled to a Simplex least-squares optimization routine. A similar approach is described in recent work by Marthinsen, Høier & Bakken (1990) and Bird & Saunders (1992). Recent improvements to the algorithm include automated beam-direction refinement and the treatment of weak beams by a perturbation Bethe potential, which will be described in a future paper. The final refinements were made using 124 dynamically interacting beams. These include all beams of appreciable intensity. Among these 124 beams, 19
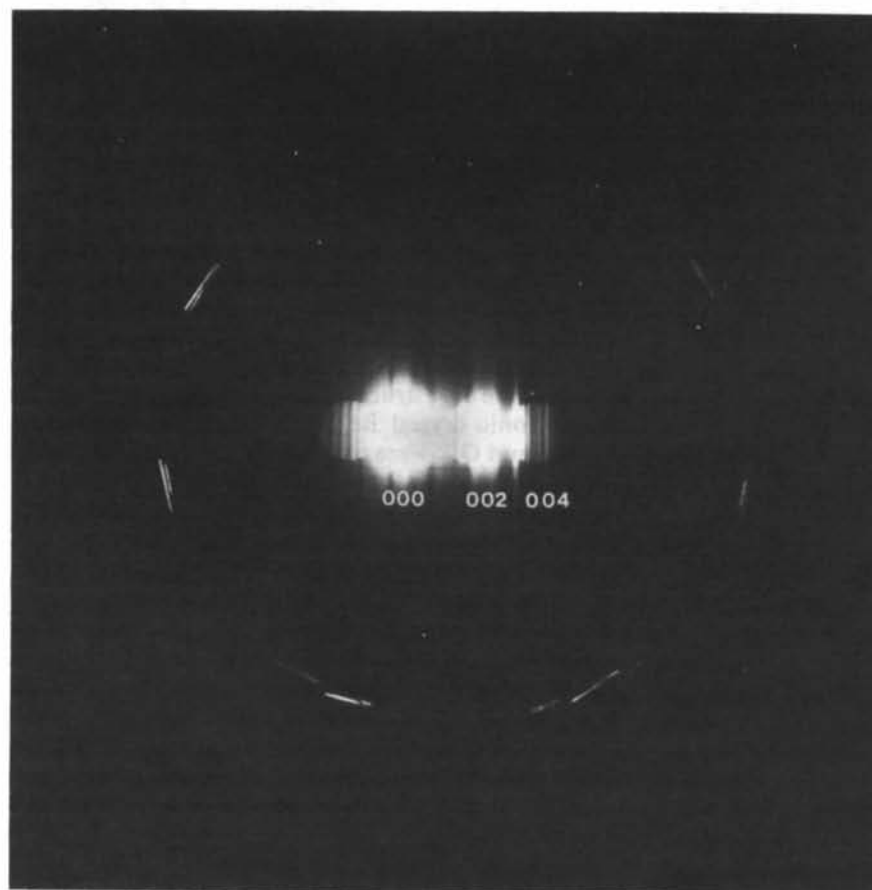

Fig. 3. This CBED pattern shows the orientation used for the analysis of Fig. 2, near the [$\bar{1}$3.0] zone axis. Different portions of the first- and second-order discs show the 00.2 and 00.4 Bragg conditions in a single recording. HOLZ reflections in this otherwise sparse zone are also seen in the bright outer ring.

strong beams with small excitation errors were treated by matrix diagonalization and the remaining weak beams treated using the Bethe perturbation potential. The Bloch-wave program used is detailed by Zuo, Gjønnes & Spence (1989), the relevant dynamical electron diffraction theory is reviewed by Humphreys (1979) and Spence & Zuo (1992) and the simplex algorithm is described by Press, Flannery, Teukolsky & Vetterling (1986) (subroutine *AMOEBA*). The overall process is similar to the Rietveld (1969) method of neutron refinement. The adjustable parameters for the refinement of an acentric crystal are: crystal thickness, complex structure factors, complex absorption coefficients and the incident-beam direction. The absorption coefficients take account of depletion of the elastic wavefield by inelastic scattering, mainly due to phonon excitation. These were taken from Bird & King (1990) but the absorption coefficient for the 002 reflection was refined. Debye–Waller factors were taken from Downs *et al.* (1985). Any error in the Debye–Waller factor will introduce a corresponding error in the converted X-ray structure factors. The z parameter was not refined. For every set of parameters required by the optimization algorithm, a matrix of structure factors and excitation errors must be diagonalized for every data point since each data point in the rocking curve corresponds to a different incident-beam direction (with different excitation errors). Because the crystal is acentric, the use of first-order perturbation theory to find changes in eigenvalues alone due to small changes in the complex potential may cause significant error in the simulation and was therefore not used (Spence & Zuo, 1992). (A full diagonalization was used instead.)

A goodness-of-fit index χ^2 was defined by

$$\chi^2 = \sum_i f_i (cI_i^{\text{theory}} - I_i^{\text{exp}})^2 / \sigma_i^2 \qquad (1)$$

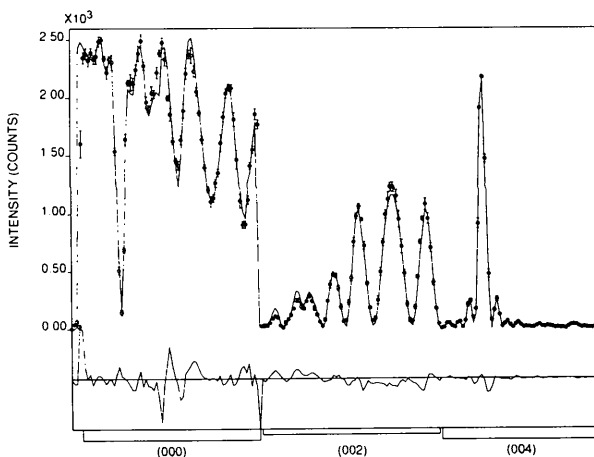and its minimum value sought using the simplex

Fig. 4. Similar to Fig. 2, but recorded for a different thickness, found after refinement to be $T = 1060.3$ Å 80 kV.

Table 1. *Comparison of experimental* BeO 002 *and* 004 *structure-factor amplitude and phase measurements* (*by both X-ray and electron-beam methods*) *with calculations*

Experiment e^- refers to our present electron diffraction measurements. Experiment X refers to our most recent X-ray results, where the phases are calculated from an electron density model. Atoms and ions are the structure factors calculated with the assumption of spherical neutral atoms and ions (Be^{2+} and O^{2-}). Scattering factors for Be^{2+} and O^{2-} were obtained from *International Tables for Crystallography* (1992) and Sanger (1969), respectively. The potential Fourier coefficient $V(002)$ is given in V, F^X in number of electrons and phases φ in rad. The agreement between the electron and X-ray phases and the increased accuracy of the electron value should be noted.

	Experiment e^-	Experiment (X)	Atoms	Ions
$\lvert F^X(002)\rvert$	11.59 (2)	11.27 (4)	10.96	11.15
$\varphi^X(002)$	−1.1900 (9)	−1.195 (44)	−1.186	−1.207
$\lvert V(002)\rvert$	5.149		5.622	5.53
$\varphi(002)$	−0.88478		−0.91646	−0.87684
$F^X(004)\rvert$			2.2377	2.0822
$\varphi^X(004)$			−2.98752	−2.98035

optimization method. Here, $f_i = 1$ for points inside the CBED disc and $f_i = 0$ for points outside the CBED disc. Also, σ_i^2 is the variance of the ith data point, which was measured using five repeated scans. (At low count rates, we find the distribution to be Poisson so that $\sigma_i^2 = I_i^{\text{exp}}$.) Furthermore, c is a normalization coefficient, which can be found either by normalizing the calculated and experimental data at a particular point or by taking the first-order derivative of χ^2. This gives

$$c = \sum_i [(f_i/\sigma_i^2) I_i^{\text{exp}} I_i^{\text{theory}}] / \sum_i [(f_i/\sigma_i^2) I_i^{\text{theory}}]. \qquad (2)$$

In the final refinement, six parameters were refined: the amplitude and phase of the 00.2 structure factor, the amplitude and phase of the 00.2 absorption coefficient, the amplitude of the 00.4 absorption coefficient and the thickness. The amplitude and phase of the 00.4 structure factor were assigned values for an ionic crystal $Be^{2+}O^{2-}$. The scattering factors for B^{2+} and O^{2-} were taken from *International Tables for Crystallography* (1992) and Sanger (1969), respectively, with the assumption of spherical atoms. These values are listed in Table 1. A similar assumption was made for the other high-order reflections. The effects of a possible error in the amplitude of the 00.4 structure factor due to the bonding effect is found to be insignificant in our refinement. However, because of the factor of 2 in the expression given above for the two-phase invariant, an error in the phase of the 00.4 structure factor will introduce an error half as great in the measurement of the 00.2 structure-factor phase.

In detail, the refinement procedure used for Fig. 2 was as follows.

1. The positions of the narrow 00.4 Bragg peaks shown in Fig. 2(*a*) were used to assign an approxi-

mate beam direction and hence an excitation error to each point of the scan. This defines the x component (along [00.1]) of the projection of the incident wave vector in the zero-order Laue zone $K_t(x)$. Seven-beam dynamical 00.h systematics calculations were then refined against this data, with use of only the crystal thickness and small changes in beam direction as refinement parameters. About 20 search steps were needed to minimize χ^2.

2. Values of the amplitude and phase of the electron structure factor $U(00.2)$, the amplitude and phase of the absorption coefficient $U'(00.2)$ and thickness were next treated as refinement parameters, again with use of only the 00.h systematics reflections in the sparse [$\bar{1}3.0$] zone. The phase of the absorption coefficient $\varphi'(00.2)$ was assumed to be -1.24 rad.

3. Steps 1 and 2 were repeated until a minimum in χ^2 was found, at $\chi^2 = 5.04$. At this point, we had $t = 709.1$ Å, $|U(00.2)| = 0.039230$, $\varphi(00.2) = -0.89719$ rad, $|U'(00.2)| - 0.000755$, $\varphi'(00.2) = -0.62$ rad and $|U'(00.4)| = 0.000159$. (All electron structure-factor values U_g are in Å^{-2}.)

4. The y coordinate of the beam direction $K_t(y)$ was determined using the micrographs (e.g. Fig. 3). (No simple features in the scans allow this to be determined easily.) From the definition of incident-beam direction given previously (Zuo & Spence, 1991), the component K_t of the wave vector drawn in the ZOLZ from the center of the [$\bar{1}3.0$] zone to the first point of the scan in Fig. 2 was found to be -1.282 g (00.2) $- 0.001$ g (31.0), while that of the last point was 1.755 g (00.2) $- 0.01$ g (31.0). All appreciable off-systematics reflections were then included in the calculations, for a total of 124 beams. The refinement was then repeated using these beams and with the complex $U(00.2)$, $U'(00.2)$, $|U'(00.4)|$ and t treated as adjustable parameters. A minimum was found at $\chi^2 = 5.04$ with the values:

$$|U(00.2)| = 0.03959\ (14)\ \text{Å}^{-2},$$

$$\varphi(00.2) = -0.885\ (17)\ \text{rad},$$

$$|U'(00.2)| = 0.00073\ (6)\ \text{Å}^{-2},$$

$$\varphi'(00.2) = -1.1\ (5)\ \text{rad},$$

$$|U'(00.4)| = 0.0002\ (1)\ \text{Å}^{-2},$$

$$t = 711.6\ (16)\ \text{Å}.$$

5. Step 4 was repeated with a different starting point and the global nature of the minimum thus confirmed. The polarity of the crystal was confirmed by repeating the analysis with every g replaced by $-$g in the computations. The result was found to increase χ^2 to about 20. The final best fit is shown in Fig. 2.

Whereas the principle of refining structure-factor amplitudes and phases from systematic rocking curves has been described previously (as have methods for refining absorption coefficients), this may be the first refinement of the phase of the absorption coefficient. In the kinematic approximation for an acentric crystal with absorption, we have

$$I_g \propto |U_g + iU'_g|^2$$
$$= \|U_g\|^2 + \|U'_g\|^2 + 2\|U_g\|\,\|U'_g\| \sin{(\varphi_g - \varphi'_g)}. \quad (3)$$

Because of the last term, there is a modification to the intensity of the rocking curve for reflection g due to the absorption phase. A similar conclusion holds in the two-beam approximation (Bird, 1990; Spence & Zuo, 1992). In X-ray diffraction, this effect is known as anomalous dispersion. Its effects in electron diffraction were pointed out by Bird (1990) and have also been observed in electron-energy-loss spectroscopy (Taftø, 1987). The effect allows the phase of the absorption coefficient to be measured from a comparison of the g and $-$g rocking-curve intensities. However, in this refinement, the intensities of reflections 0 and g are compared to refine the phase of the absorption potential.

Fig. 4 shows a scan from a different region of the crystal, which has a different thickness. It was refined using the same procedure as above and shows the data and the best fit. The results of the refinement were

$$|U(00.2)| = 0.03982\ (13)\ \text{Å}^{-2},$$

$$\varphi(00.2) = -0.879\ (17)\ \text{rad},$$

$$|U'(00.2)| = 0.00090\ (7)\ \text{Å}^{-2},$$

$$\varphi'(00.2) = -0.4\ (5)\ \text{rad},$$

$$|U'(00.4)| = 0.00004\ (10)\ \text{Å}^{-2},$$

$$t = 1059.7\ (20)\ \text{Å}.$$

These fall within the error ranges of the previous analysis, giving considerable confidence in our method.

These electron structure-factor measurements may be converted into X-ray structure factors at room temperature using the Mott–Bethe formula (Humphreys, 1979). Firstly, we have

$$U_g = \gamma F_g^B / \pi\Omega = 2m\|e\|\,V_g / h^2, \quad (4)$$

where γ is the relativistic constant, Ω the unit-cell volume and F_g^B the electron structure factor evaluated in the first Born approximation. Since the crystal potential (with Fourier coefficients V_g in V) is related to the charge density by Poisson's equation, we may obtain the X-ray structure factor F_g^X from U_g as follows:

$$F_g^X = \sum_i Z_i \exp{(-B_i S^2)} \exp{(2\pi i g \cdot r)}$$
$$- (8\pi^2 \varepsilon_0 h^2 \Omega S^2 / \gamma m_e e^2)\, U_g \quad (5)$$

$$= \sum_i Z_i \exp{(-BS^2)} \exp{(2\pi i g \cdot r)}$$

$$- CX^2 \Omega U_g / \gamma. \quad (6)$$

Here the numerical constant $C = 131.2625$ if A, Ω and $U_{\mathbf{g}}$ are given in Å units. Exchange and virtual inelastic corrections to the potential have been shown to be negligible (Humphreys, 1979), ensuring that Poisson's equation may be applied.

Using these expressions, we obtain from our refinements of Fig. 2

$$|F^X(00.2)| = 11.59\,(2)\,\text{e}$$

and

$$\varphi^X(00.2) = -1.190\,(9)\,\text{rad},$$

where $\varphi^X(00.2) = -1.190\,(9)$ rad, is the phase of $F^X(00.2)$ calculated with respect to an origin at a Be-atom site.

4. Discussion

In Table 1, we compare our results with calculated results for spherical atoms and ions using the atomic scattering factors from *International Tables for Crystallography* (1992) and the atomic scattering factor for O^{2-} from Sanger (1969). The crystal data are taken from Downs *et al.* (1985) and the Debye–Waller factors used were $B_{Be} = 0.355$ and $B_O = 0.28$ Å^2. Also included in Table 1 are the results of X-ray measurements for the same structure factor, in good agreement. The value of the phase given $(-1.195$ rad) was computed from a multipole refinement. A generalized scattering-factor model was fitted to 104 single-crystal X-ray structure-factor moduli collected from a crystal of the same batch as those used for the γ-ray (Downs *et al.*, 1985) and electron diffraction work. The atomic scattering factors for Be and O were given by a multipole expansion at the hexadecapole level (Stewart, 1976). Generalized scattering factors (g.s.f.s) were taken from a multipole expansion of the molecular form factor for diatomic BeO calculated from a Hartree–Fock wave function. An eight exponential fit was used for the monopole g.s.f.s and single exponential fits were used for the higher multipoles. Radial parameters are not refined. The final agreement factor

$$R = \sum \|F_o| - |F_c\|/\sum |F_o| = 0.71\%.$$

We note that the standard deviation of the phase derived from this refinement was about 50 times that of the electron diffraction result. Both the X-ray and the electron diffraction results for the 00.2 phase lie between calculations for free neutral atoms and those for ions.

In conclusion, it appears that the convergent-beam electron diffraction technique may be the most accurate method for the measurement of low-order structure-factor phases from acentric crystals with small unit cells. For amplitudes, the method is somewhat less accurate than the best values for silicon obtained by the X-ray *Pendellösung* method. Our result for the

amplitude of the 00.2 structure factor differs somewhat from previous X-ray measurements. Our three-beam electron diffraction phase measurements are substantially more accurate than values derived from X-ray amplitude measurements. The method may therefore allow the extension of previous highly accurate studies of charge density in silicon to acentric crystals from which large single crystals cannot be grown. For acentric crystals for which large single crystals can be grown (such as the wurtzite-$2H$ compound semiconductors), charge-density studies might be based on a combination of X-ray and electron diffraction results.

References

BIRD, D. (1990). *Acta Cryst.* A **46**, 208–214.
BIRD, D. & JAMES, R. (1988). *Ultramicroscopy*, **26**, 31–35.
BIRD, D. & KING, Q. A. (1990). *Acta Cryst.* A46, 202–208.
BIRD, D. & SAUNDERS, M. (1992). *Acta Cryst.* A48, 555–561.
CHANG, S.-L. (1987). *Crystallogr. Rev.* **1**, 87–189.
COWLEY, J. M. (1992). Editor. *Techniques of Transmission Electron Diffraction.* Oxford Univ. Press.
DOWNS, J. W., ROSS, F. K. & GIBBS, G. V. (1985). *Acta Cryst.* B41, 425–431.
EADES, J. A. (1988). In *Microbeam Analysis*, edited by D. E. NEWBURY. San Francisco Press.
GJØNNES, J. & MOODIE, A. F. (1965). *Acta Cryst.* **19**, 65–67.
HÜMMER, K., WECKERT, E. & BONDZA, H. (1990). *Acta Cryst.* A46, 393–402.
HUMPHREYS, C. J. (1979). *Rep. Prog. Phys.* **42**, 1825–1887.
ICHIMIYA, A. & UYEDA, R. (1977). *Z. Naturforsch. Teil A*, **32**, 750–753.
International Tables for Crystallography (1992). Vol. C, p. 488. Dordrecht: Kluwer Academic Publishers.
KAMBE, K. (1957). *J. Phys. Soc. Jpn*, **12**, 1–7.
MARTHINSEN, K. & HØIER, R. (1986). *Acta Cryst.* A42, 484–492.
MARTHINSEN, K. & HØIER, R. (1988). *Acta Cryst.* A44, 558–562.
MARTHINSEN, K. & HØIER, R. (1989). In *Proc. Electron Microscopy Society of America*, edited by G. W. BAILEY. San Francisco Press.
MARTHINSEN, K., HØIER, R. & BAKKEN, L. (1990). In *Proc. 12th International Congress on Electron Microscopy*, pp. 492–493. San Francisco Press.
MARTHINSEN, K., MATSUHATA, H., HØIER, R. & GJØNNES, J. (1988). *Aust. J. Phys.* **41**, 449–453.
MAYER, J., SPENCE, J. C. H. & MOBUS, G. (1991). In *Proc. Electron Microscopy Society of America*, edited by G. W. BAILEY. San Francisco Press.
PRESS, W. H., FLANNERY, B., TEUKOLSKY, S. & VETTERLING, W. (1986). *Numerical Recipes.* Cambridge Univ. Press.
RIETVELD, H. M. (1969). *J. Appl. Cryst.* **2**, 65–71.
SANGER, P. L. (1969). *Acta Cryst.* A25, 694–702.
SHEN, Q. & COLLELA, R. (1988). *Acta Cryst.* A44, 17–28.
SPENCE, J. C. H. (1993). *Acta Cryst.* A49, 231–260.
SPENCE, J. C. H. & ZUO, J. M. (1992). *Electron Microdiffraction.* New York: Plenum.
STEWART, R. F. (1976). *Acta Cryst.* A32, 565–574.
TAFTØ, J. (1987). *Acta Cryst.* A43, 208–211.

THORKILDSEN, G. (1987). *Acta Cryst.* A43, 361–369.
VIDAL-VALAT, G., VIDAL, J. P., KURKI-SUONIO, K. & KURKI-SUONIO, R. (1987). *Acta Cryst.* A43, 540–550.
WECKERT, E. & HÜMMER, K. (1990). *Acta Cryst.* A46, 387–393.
ZUO, J. M., GJØNNES, K. & SPENCE, J. C. H. (1989). *J. Electron Microsc. Tech.* 12, 29–33.

ZUO, J. M., HØIER, R. & SPENCE, J. C. H. (1989). *Acta Cryst.* A45, 839–855.
ZUO, J. M. & SPENCE, J. C. H. (1991). *Ultramicroscopy*, 35, 185–193.
ZUO, J. M., SPENCE, J. C. H. & HØIER, R. (1989). *Phys. Rev. Lett.* 62, 547–550.

Automated Structure-Factor Refinement from Convergent-Beam Electron Diffraction Patterns

By J. M. Zuo

Physics Department, Arizona State University, Tempe, AZ 85287, USA

Abstract

An improved algorithm is described for automated structure-factor refinement using convergent-beam electron diffraction patterns. In addition to refinement of structure factors, absorption coefficients and sample thickness, the new algorithm includes beam-direction refinement, the inclusion of weak-beam effects using the Bethe potential and the inclusion of finite-sized detector effects. The use of these new features is illustrated through the refinement of the MgO 200 systematic reflections.

1. Introduction

Convergent-beam electron diffraction (CBED) is a highly efficient structural probe – a large amount of quantitative structural and compositional information may be obtained from volumes as small as 1 nm in diameter. There has been continuous interest recently in devising systematic methods to extract this information from the readily available CBED patterns (for a recent review, see Spence, 1993). Most recently, Zuo & Spence (1991) used numerical optimization methods to automate the process of comparing elastic-filtered CBED intensities with Bloch-wave calculations, while treating structure factors, absorption coefficients and thickness as adjustable parameters. Similar methods may be used to compare experimental high-order Laue-zone (HOLZ) patterns with kinematical simulations, with the lattice parameters treated as adjustable parameters (Zuo, 1992a). The structure factors give compositional and structural information on the crystal, while the lattice parameters give local strain information. There have been many other efforts to extract information from CBED patterns using optimization methods. These include the theoretical studies by Marthinsen, Høier & Bakken (1990) on the refinement of structure-factor amplitude and phase from non-systematic CBED patterns, studies by Bird & Saunders (1992) on the possibility of determining crystal structure from zone-axis CBED patterns, and the experimental measurement of atomic positions from zone-axis HOLZ intensities by Tanaka & Terauchi (1990). The earlier automated refinement method described by Zuo & Spence (1991) was effective in refining complex structure factors and thickness, but required tedious precise orientation matching and has since been improved in several ways. These include an algorithm for automated beam-direction refinement, which was not available previously. The other new feature is a modification of the original algorithm to allow weak beams to be treated by the Bethe-potential method (Bethe, 1928). The Bethe-potential method was chosen over the perturbation method (Eaglesham, 1989; Zuo, 1991) because it has the advantages of simplicity and speed (Zuo, 1992b). This new feature allows us to include weak beams in the simulation to improve the convergence and requires only a fraction of the computer time compared to diagonalizing a full matrix with the weak beams included. The third new feature is an algorithm to include detector effects in the simulation and thus reduce possible systematic errors in the measured experimental data. These new features will be discussed in the following sections. Before doing so, the results of earlier work will be briefly summarized.

In a previous paper (Zuo & Spence, 1991), the algorithm *REFINE/CB* was described for automation of the process of measuring structure factors, absorption coefficients and thickness from energy-filtered convergent-beam electron diffraction data in the systematics orientation. This was accomplished by the definition of a best-fit parameter (χ^2) and use